Contents lists available at ScienceDirect

Electrochimica Acta

CrossMark

The impedance response of different mechanisms for LiCoO$_2$/acetylene carbon electrodes in alkaline solutions under polarization conditions

Homero Castaneda [*],[1]

National Center for Education and Research in Corrosion and Materials Reliability, Chemical and Biomolecular Engineering Department, The University of Akron, Akron, OH, United States

ARTICLE INFO

ABSTRACT

The kinetics of LiCoO$_2$ electrodes with different carbon ratios in alkaline aqueous solutions was studied by electrochemical impedance spectroscopy (EIS) and cyclic voltammetry (CV). The composition of the electrode influences the mechanism controlling the interface. The redox reactions identified by CV indicated the potential regions where the charge transfer process is the dominant mechanism. EIS in (Li$_2$SO$_4$ + LiOH) alkaline solutions characterized different interfacial mechanisms when potential bias was applied to electrodes formed with different acetylene carbon (AC)/LiCoO$_2$ ratios. The different carbon/active ratios revealed different interfacial characteristics due to the cylindrical porous distribution of the composite electrode. DC and AC techniques were performed to characterize the interfacial mechanisms influenced by composite ratio, particle geometry and distribution under bias conditions. Transmission line modeling (TLM) was used to characterize the impedance signal resulting from the physical parameters influencing the mechanisms occurring at the porous composite layer/electrolyte interface. Interfacial mechanisms associated with TLM elements helped to quantitatively characterize the functionality of the different LiCoO$_2$/AC ratios present in the electrode compositions. The proposed TL model was validated with the experimental data and high surface characterization, resulting in good agreement.

1. Introduction

LiCoO$_2$ electrodes have been used in lithium-ion batteries due to their stability, energy density, and voltage among different parameters [1]. The mechanisms and performance of these electrodes in different organic and aqueous electrolytes have been studied in various previous works [2]. Even though organic electrolytes provide a higher voltage window than aqueous electrolytes, aqueous electrolytes have resurged due to safety issues that can occur [3] when organic electrolytes are used in various energy storage applications [3–5]. Electrodes made with LiCoO$_2$, acetylene carbon (AC), and polymer binders have demonstrated interfacial characteristics in aqueous electrolytes [4,5] that are similar to those found in organic electrolytes. The favorable interfacial properties of the LiCoO$_2$ electrode have resulted in the fabrication and characterization of new electrode formulations.

Because porous electrodes have an active surface that is readily available for suitable reactions and mechanisms, they have been developed for storage devices. The particle size, composition, and distribution are some parameters that affect the interfacial mechanisms and transport in the presence of different electrolytes. Recent efforts focused on ultrafine powders have revealed that electrochemical performance varies with particle size [6,7]. In contrast, some authors found that larger particle size provided benefits such as enhanced battery operation, better cycle life, and larger specific capacitance in lithium batteries. Effects on geometry and particle distribution electrodes have also been studied for their capacitance behavior of bounded diffusion and their relationship with impedance properties [8,9]. The solid surface produced by the pore geometry, particle distribution, and chemistry when composite electrodes are synthetized impacts the mechanisms at each formed interface.

Antolini [10] comprehensively reviewed the performance of different solid state forms of LiCoO$_2$ based on the synthesis route and the oxide phase present in the material. The structural differences between the resulting phases controlled the kinetics of the reversible faradic reactions and surface processes. The low-temperature spinel cubic structure is characteristic of lithiated synthesis processes. The high-temperature hexagonal and layered structures exhibit kinetics that is influenced by the particle size [11]. The disorder introduced by structural defects is recognized to

* Tel.: +1 3309727398; fax: +1 3309725856.
E-mail address: homeroc@uakron.edu
[1] ISE member.

Z_p	impedance per pore
n	number of pores
Z_T	total impedance
R_m	resistance of the composite material
R_s	resistance of the electrolyte
l	length of the pore
Z_{tm}	mass transfer impedance
Z_{ct}	charge transfer impedance
C	defined parameter equal to $\cosh(\tau^{0.5}l)$
S	defined parameter equal to $\sinh(\tau^{0.5}l)$
δ	defined parameter equal to $((R_m + R_s)/Z_{tm})$
τ	defined parameter equal to $((R_m + R_s)/Z_{ct})$
R_p	charge transfer mechanism resistance
α_{ct}	dispersion or roughness factor
Q_p	constant phase element
ω	frequency
Z_{tm}	total impedance for active–passive processes in transmission line
R_{ct}	charge transfer resistance attributable to vacancy or intercalation process
C_{dl}	constant phase element
α_{tm}	constant associated with porous $LiCoO_2$/AC layer roughness
Z_w	Warburg impedance
σ	magnitude in the real and imaginary component for infinite constant reaction rate (fully controlled by mass transfer)
ΔV	potential applied
n_t	number of electrons transferred
F	Faraday constant
A	area of the composite electrode
C_s	lithium ionic concentration of the mass transfer species
D	diffusion coefficient of the ionic species
Z_w	Warburg impedance
Z_{ap}	impedance influenced by the active/outer surface and charge/mass transfer state
ϕ	charge/mass transfer mechanism ratio
Z_{TMo}	total impedance based on a combined transport mechanisms
n	number of pores
σ_R	real mass transfer magnitude
σ_{im}	imaginary mass transfer magnitude
$Z_{Tp,real}$	real impedance
$Z_{Tp,im}$	imaginary impedance
$Z_{exp,real}$	real magnitude in experimental impedance.
$Z_{exp,im}$	imaginary magnitude in experimental impedance.
$\Delta Z_{real,(\omega)}$	gradient difference of calculated minus experimental real impedance per frequency
$\Delta Z_{im,(\omega)}$	gradient difference of calculated minus experimental imaginary impedance per frequency

Fig. 1. Top view: 100AC composite.

$LiCoO_2$ structural changes (faradic) were observed. The reversible process was attributed to the faradic processes that occurred at the composite layer/electrolyte interface. The electrochemical mechanisms were used to identify and characterize the physical and chemical effect in the porous composite electrodes. The electrodes were fabricated with different AC/$LiCoO_2$ ratios. The carbon black (AC) favored the double-layer behavior and intercalation processes, whereas the $LiCoO_2$ influenced the reversible (or faradic) phase transformation processes. Different bias potentials were used to characterize the interface by electrochemical impedance spectroscopy (EIS). The experimental results assisted with the correlation of the interfacial mechanisms based on the chemical composition. The theoretical approach considered the electrode to be a porous layer forming a transmission line (TL). The TL modeling (TLM) application showed that if each element with interfacial processes can be defined, the relationship between the physical and chemical properties of the solid state layer could be quantified.

2. Experimental

2.1. High resolution characterization

The synthesis of the stoichiometric $LiCoO_2$ composite materials was carried out as previously described [12]. Scanning electron microscopy of the composite electrode material was resolved for different ratios using a JEOL microscope at 30 kV. Fig. 1 shows the top and lateral view of different pore distributions for different material compositions. The top view of the pore distribution is shown in Figs. 1–3 for the 100% AC, $LiCoO_2$/AC (80/20) ratio and 100% $LiCoO_2$ electrode materials, respectively. Fig. 4 shows the lateral view of the 100% $LiCoO_2$ electrode.

2.2. Morphology description

Fig. 1 shows the top view of the AC electrode $LiCoO_2$/AC (0/100) with the 5% PTFE (polytetrafluoroethylene) binder particles that formed cylindrical pores with diameters close to 0.4 μm; the particle distribution is closely packed due to the small diameter particles. Small diameter particles (approximately 0.1 μm) and white particles are related to the PTFE binders. The top view in Fig. 2 reveals that in the $LiCoO_2$/AC (80/20) pore distribution, no agglomeration texture is evident. When AC was added, the particle distribution was altered, with pores showing a larger diameter and a denser packing configuration. The pore diameter was close to

be more stable to the intercalation/deintercalation of Li ions. The disorder can be obtained by cation or anion non-stoichiometry, ion mixing, and layering. Many efforts have been devoted to quantitatively correlate structural disordering with reversible processes, such as Li intercalation/deintercalation in the charge and discharge process [10]. Song and Bazanta [8] attributed the combined mechanism of bounded diffusion and capacitance to particle geometry and distribution due to thin layers and short diffusion lengths.

In this work, we present electrochemical test results for electrodes fabricated from a high-temperature $LiCoO_2$ layered structure. Three cathodic 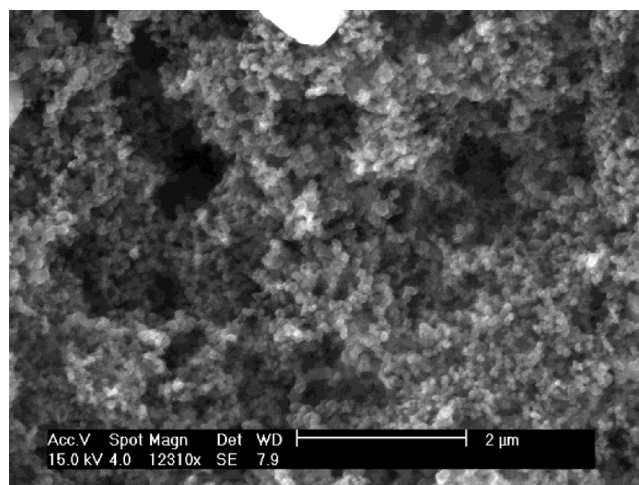and anodic peaks corresponding to the